Drug Design, Development and Therapy

Dovepress
open access to scientific and medical research

Open Access Full Text Article

ORIGINAL RESEARCH

Panax quinquefolium L. and *Salvia miltiorrhiza* Bunge. Enhances Angiogenesis by Regulating the miR-155-5p/HIF-1α/VEGF Axis in Acute Myocardial Infarction

Xingxing Li[1], Rongpeng Liu[1], Wei Liu[1], Xin Liu[2], Zongjing Fan[1], Jie Cui[1], Yang Wu[1], Huijun Yin[3], Quan Lin[1]

[1]Dongfang Hospital, Beijing University of Chinese Medicine, Beijing, 100078, People's Republic of China; [2]The Third Affiliated Hospital, Beijing University of Chinese Medicine, Beijing, 100029, People's Republic of China; [3]Xiyuan Hospital, China Academy of Chinese Medical Sciences, Beijing, 100091, People's Republic of China

Correspondence: Quan Lin, Dongfang Hospital, Beijing University of Chinese Medicine, No. 6, Fangxingyuan District 1, Fengtai District, Beijing, 100078, People's Republic of China, Tel +86-10-67689757, Email linquanys@163.com

Background: Combination of *Panax quinquefolium* L and *Salvia miltiorrhiza* Bunge. (PS) has been widely used in the clinical treatment of ischemic heart disease. The purpose of this study was to explore the therapeutic effect and mechanism of PS on angiogenesis in rats after acute myocardial infarction (AMI).

Methods: A rat model of AMI was established by ligating the left anterior descending (LAD) artery. The grouping and administration scheme were as follows: sham group, model group, PS low-dose (PS-L) group, PS high-dose (PS-H) group, PX-478 group and angiotensin converting enzyme inhibitor (ACEI) group. After 28 days of treatment, echocardiography, myocardial infarct size, some angiogenesis markers and the miR-155-5p/HIF-1α/VEGF axis were measured.

Results: PS improved cardiac structure and function, reduced infarct size, and alleviated myocardial fibrosis and inflammatory cell infiltration in AMI rats. Mechanistically, PS enhanced the expression of HGF and bFGF in serum, increased the levels of MVD and CD31 in myocardial tissues, and inhibited the activation of the miR-155-5p/HIF-1α/VEGF pathway, which ultimately promoted angiogenesis. In addition, the regulatory effect of PS on angiogenesis was partly abolished by PX-478.

Conclusion: PS increased the expression of MVD and CD31 in the myocardium and stimulated angiogenesis. The above effects of PS may be associated with the inhibition of the miR-155-5p/HIF-1α/VEGF axis.

Keywords: *Panax quinquefolium* L, *Salvia miltiorrhiza* Bunge, angiogenesis, acute myocardial infarction, miR-155-5p/HIF-1α/VEGF

Introduction

Cardiovascular disease (CVD) is the main cause of death worldwide, leading to 17.8 million global deaths in 2017, which contributes obviously to the global health burden.[1] Acute myocardial infarction (AMI) is one of the most fatal CVDs and is caused by a sudden disruption of blood flow to the myocardium, with high rates of morbidity and mortality.[2] Since the pathological feature of AMI is poor cardiac blood perfusion, restoring blood flow is the most effective means to limit the damage to ischemic tissues. Currently, surgical techniques for restoring blood circulation reconstruction and catheter-based interventions have become increasingly prevalent, but a proportion of patients are ineligible for such treatment.[3] Thus, how to effectively achieve the goal of reducing myocardial injury after AMI, relieving symptoms, restoring cardiac function and reducing mortality has faced severe challenges.

Angiogenesis plays an important role in restoring blood supply to ischemic tissues and has taken on the emerging research area of treatment for ischemic myocardial injury after AMI.[4] Enhancing angiogenesis to improve myocardial ischemia after AMI can improve cardiac function and reduce major adverse cardiac events.[5] The enhancement of

Received: 16 June 2023
Accepted: 23 October 2023
Published: 7 November 2023

Graphical Abstract

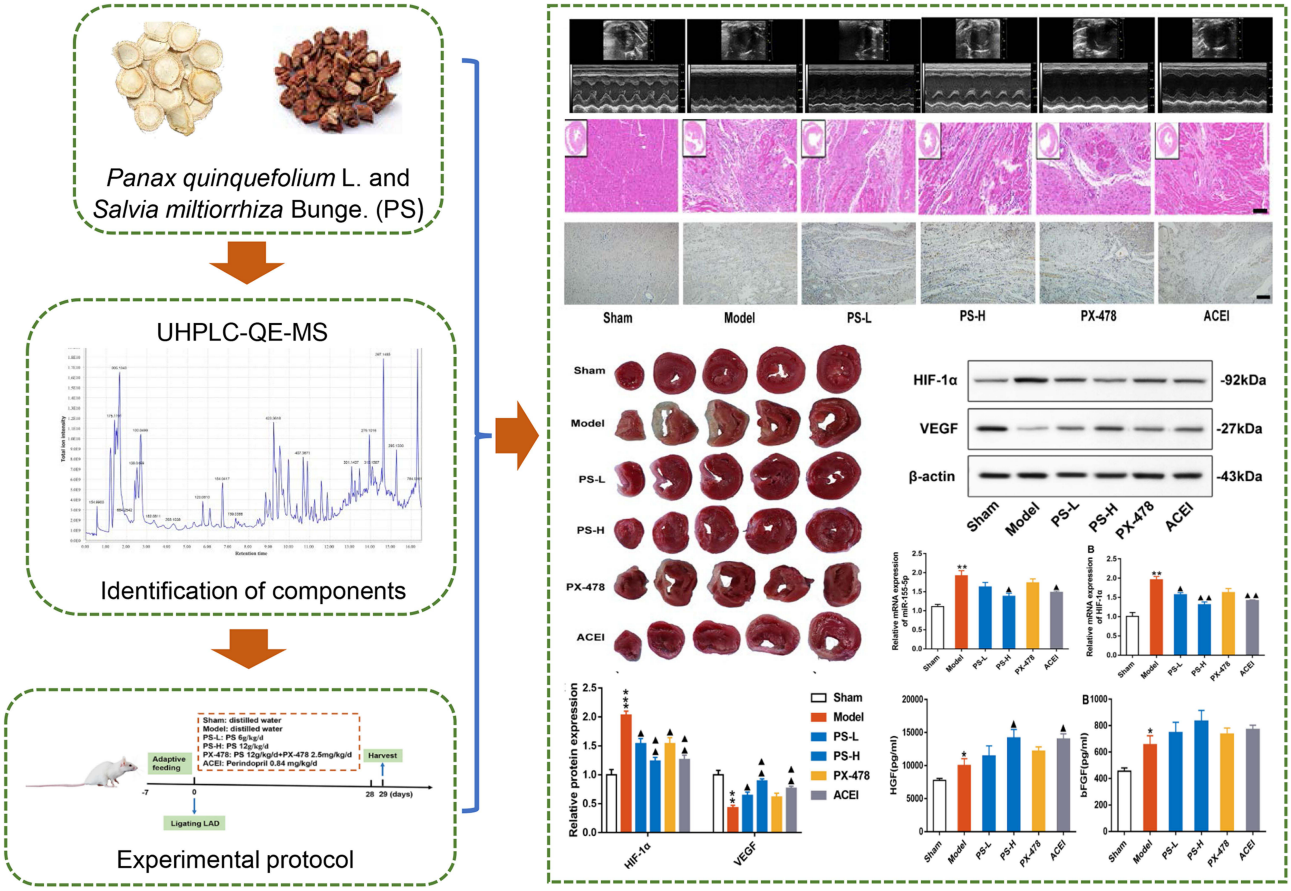

myocardial angiogenesis through therapeutic angiogenesis is a pivotal treatment strategy after AMI. Microvascular density (MVD) and CD31 are useful metrics for quantifying the extent of angiogenesis in ischemic myocardium.[6,7]

MicroRNA (miRNA) is reported to be involved in cell division, differentiation and survival.[8,9] As a multifunctional miRNA, miR-155 has been proved to be significantly upregulated in the ischemic area of AMI and involved in the pathophysiological process of angiogenesis.[10] Hypoxia inducible factor (HIF) is a transcription factor that responds to hypoxia in the cell environment.[11] HIF-1 signaling cascade mediates the effect of hypoxia on cells and plays the role of angiogenesis, in which HIF-1α is its active subunit.[12] HIF-1α maintains low concentration in cells under normal oxygen concentration due to degradation by 26S proteasome[13] and keeps stable and not be degraded by proteasome, thus activating downstream gene transcription in hypoxia.[14] Additionally, vascular endothelial growth factor (VEGF) and fibroblast growth factor (FGF) are genes that induce angiogenesis in ischemic tissues.[15] miR-155 is an upstream regulatory gene of HIF-1, which directly affects the activation of HIF-1 and regulates endothelial cells proliferation and angiogenesis.[16–18] The miR-155/HIF-1/VEGF pathway is reported to play an important role in myocardial angiogenesis, which may contribute to vascular repair after AMI.[19]

The traditional Chinese medicine (TCM) formula of *Panax quinquefolium* L and *Salvia miltiorrhiza* Bunge. (PS) has an effect of replenishing Qi and activating blood, and has been widely used to treat CVD. Our previous studies revealed that PS in a ratio of 1:3 not only inhibited carotid artery thrombosis model in rats but also stabilize vulnerable atherosclerotic plaques by inhibiting inflammatory reaction, improving oxidative stress, reducing endothelial damage and reducing lipid deposition and plaque area.[20–23] In parallel, our network pharmacology study showed that HIF-1 is the

main pathway of PS in treating coronary heart disease, and VEGF is the key target, which is related to promoting angiogenesis.[24] We thereby proposed a hypothesis that PS may promote angiogenesis by regulating miR-155-5p/HIF-1α/VEGF pathway, reduce myocardial infarct size, and improve cardiac function in AMI rats.

Materials and Methods

Materials

Perindopril was bought from Servier (Tianjin) Pharmaceuticals Ltd. (H20034053). PX-478 was purchased by Shanghai Haoyuan Biotechnology Co., Ltd (685898-44-6). ELISA Kit HGF (EK3H01) was purchased from Multisciences (China), and bFGF from Elabscience (China). Antibodies HIF-1α (ab179483-10), VEGF (EPR20705), MVD (ab198823) and CD31 (ab222783) were available from Abcam (Cambridge, United States). Anti-β-actin (sc-47778) was issued from Santa Cruz Biotechnology (Santa Cruz, California). Trizol (10296028) was offered by Invitrogen (USA). UltraPure Agarose (16500100), SuperScript III RT kit (11752050) and SYBR qpcr mix (4472920) were obtained by ABI-invitrogen (USA). Radioimmunoprecipitation (RIPA) (MDL91201), phenylmethanesulfonyl fluoride (PSMF) (MD912893) and bicinchoninic acid assay (BCA) protein assay kit (MD913053) were purchased from Medical Discovery Leader (China). The polyvinylidene difluoride membrane (PVDF) (ISEQ00010) was provided by Millipore (USA). 1% 2,3,5-triphenyltetrazolium chloride (TTC) (G1017-100 ML) was offered by Servicebio Biotechnology Co., Ltd (China). The acetonitrile (75-05-8) was obtained from Thermo (USA). The formic acid (64-18-6) was acquired from Tokyo Chemical Industry (Japan). The ammonium formate (540-69-2) was obtained from Sigma (Germany).

Methods

Preparation of PS

Panax quinquefolium L (Lot no. 22020061) and *Salvia miltiorrhiza* Bunge. (Lot no. 22025671) were recruited from Beijing Kangrentang Pharmaceutical Co., Ltd. (Beijing, China). One dosage of PS is composed of *Panax quinquefolium* L. 10 g and *Salvia miltiorrhiza* Bunge. 30 g. PS were extracted by decoction and prepared via concentration and dryness into granules. This scheme was applied by the Pharmacy Department of Dongfang Hospital, Beijing University of Chinese Medicine (Beijing, China) with reference to Good Manufacturing Practice for Drugs to guarantee the quality.

Identification of Major Chemical Components in PS

Ultra-high-performance liquid chromatography tandem mass spectrometry (UHPLC-MS/MS) was used to determine the chemical components of PS. UHPLC was made on Vanquish system (Thermo Fisher Scientific, USA). For UHPLC-ESI (+)-MS analysis, the mobile phase consists of A (acetonitrile with 0.1% formic acid) and B (H_2O with 0.1% formic acid). The elution process was as follows: 0–1 min, 2% A and 98% B; 1–9 min, 50% A and 50% B; 9–12 min, 60% A and 40% B; 12–13.5 min, 98% A and B; 13.5–14 min, 98% A and 2% B; 14–20 min, 2% A and 98% B. For UHPLC-ESI (-)-MS analysis, the analytes were carried out with (A) acetonitrile and (B) ammonium formate (5mM). The elution process was as follows: 0–1 min, 2% A and 98% B; 1–9 min, 50% A and 50% B; 9–12 min, 60% A and 40% B; 12–13.5 min, 98% A and 2% B; 13.5–14 min, 98% A and 2% B; 14–17 min, 2% A and 98% B.

MS was conducted on Q Exactive (Thermo Fisher Scientific, USA) with ESI ion source according to certain conditions and parameters.

Animals

Sprague-Dawley (SD) rats (200 ± 20 g, male) were obtained by Beijing Vital River Laboratory Animal Technology Co. Ltd. (License No. SCXK, 2016-0011, Beijing). These animals were housed in specific-pathogen-free (SPF) environment during a 12:12 h light/dark cycle, controlled temperature of 22 ± 1°C, and humidity of 50 ± 10%. Our experiment was subject to approval by the Animal Ethics Committee of Dongfang Hospital, Beijing University of Chinese Medicine (DFYY202221R) and adhered to the National Institutes of Health Guidelines on Laboratory Research.

Establishment of AMI Models

The AMI rat models were established through ligating the left anterior descending (LAD) after 7 days of adaptive feeding.[25] Briefly, rats were anesthetized with 1% pentobarbital sodium and ventilated with ventilator. A left thoracotomy

was performed along the third and fourth intercostals to expose the heart, then LAD was ligated with suture. After operation, 60,000 U/d penicillin was injected intramuscularly for 3 days to avoid infection. Sham surgery experienced the same process except for LAD ligation.

Animal Grouping and Intervention

Rats were randomly divided into six groups (n=12 per group): (a) sham group: distilled water, intragastric administration, once daily; (b) model group: distilled water, intragastric administration, once daily; (c) PS low-dose (PS-L) group: *Panax quinquefolium* L. 1.5 g/kg/d, *Salvia miltiorrhiza* Bunge. 4.5 g/kg/d, intragastric administration, once daily; (d) PS high-dose (PS-H) group: *Panax quinquefolium* L. 3 g/kg/d, *Salvia miltiorrhiza* Bunge. 9 g/kg/d, intragastric administration, once daily; (e) PX-478 group: *Panax quinquefolium* L. 3 g/kg/d, *Salvia miltiorrhiza* Bunge. 9 g/kg/d, intragastric administration, once daily; PX-478 2.5 mg/kg/d, intraperitoneal injection, once a week; (f) angiotensin converting enzyme inhibitor (ACEI) group: Perindopril 0.84 mg/kg/d, intragastric administration, once daily. The intervention was initiated on the second day after operation for 4 weeks in each group. In this study, the experimental doses were calculated based on body surface area.

Echocardiography

After 4 weeks of treatment, all rats were anesthetized for echocardiography. M-mode echocardiography was used to evaluate the heart movement after positioning the rat heart with high-frequency probe, and the average value of 3 cardiac cycles was taken for each rat. Left ventricular ejection fraction (LVEF), left ventricular fractional shortening (LVFS), left ventricular anterior wall in diastole (LVAWd), left ventricular anterior wall in systole (LVAWs), left ventricular end-diastolic inner diameter (LVIDd), left ventricular end-systolic inner diameter (LVIDs), left ventricular posterior wall in diastole (LVPWd) and left ventricular posterior wall in systole (LVPWs) were detected to assess cardiac structure and function.

Sample Collection

After 4 weeks of intervention and echocardiography, blood and the heart were gathered in rats. Blood samples were harvested from abdominal aorta and centrifuged to obtain serum (3000 rpm, 15 min, 4°C). The serum was kept at −80°C. Then the heart was immediately extracted. The complete heart was only used for TTC experiments. A portion of the marginal zone of myocardial infarction was fixed with 4% paraformaldehyde for histopathological examinations. The remaining ischemic myocardial tissue was minced by scissors and stored at −80°C for further molecular biological experiments.

Histological Analysis

After dewaxing and dehydration, the heart paraffin sections were stained with hematoxylin/eosin (H&E) or Masson staining kit to measure pathological changes. Finally, the sections were sealed with neutral gum and photographed under an optical microscope.

The hearts were derived from rats and immediately rinsed in phosphate-buffered saline (PBS). Afterwards, the hearts were stored at −80°C for 30 min and cut into 5 slices below the ligature. The prepared sections were incubated with TTC at 37°C and avoided light for 20 min, and then fixed with 10% formalin for 4 h. The infarcted area was white and quantified using Image J software.

Immunohistochemistry

The expression of CD31 and MVD in ischemic myocardial tissues of AMI rats were monitored by immunohistochemistry. The prepared heart paraffin sections were dewaxed by gradient ethanol to water (the same as histopathological staining). Subsequently, the sections were submitted to antigen repair, blocked using serum, and incubated with primary and secondary antibody, and then observed under the optical microscope. Finally, the image J software was used for quantization.

Enzyme-Linked Immunosorbent Assay

Enzyme-linked immunosorbent assay (ELISA) were used to evaluate the levels of HGF and bFGF in the serum of rats. After sample addition, incubation, plate washing, incubation of primary and secondary antibodies, coloration and termination, the optical density (OD) of each sample was immediately measured with the microplate reader at 450 nm. The sample concentration was estimated according to the OD value and standard curve.

Real-Time Quantitative PCR

Total mRNA of myocardial tissue was extracted by Trizol method. The qualified mRNA was reverse transcription into cDNA with SuperScript III RT kit. Then, cDNA amplification was done with SYBR qpcr mix. The RT-qPCR conditions were as follows: 95°C for 5 min, then 40 cycles of 95°C for 10s, 20s at 58°C and 72°C for 20s, subsequent 95°C for 10s and 60°C for 60s. Finally, it ends at 95°C for 15s. The mRNA levels of miR-155-5p, HIF-1α and VEGF in myocardial tissue of rats were detected by Real-time quantitative PCR (RT-qPCR). The relative mRNA levels for miR-155-5p, HIF-1α and VEGF was analyzed by the $2^{-\Delta\Delta Ct}$ method. Primers are given in Table 1.

Western Blot Assay

Myocardial tissues were lysed in RIPA buffer with PMSF to produce the homogenate. Total protein levels were quantified by BCA kit. The protein samples were loaded and electrophoresed on 10% sodium dodecyl sulfate-polyacrylamide gel (SDS-PAGE) and transferred to a PVDF. After sealing, incubation of primary and secondary antibodies and exposure, the protein levels of HIF-1α and VEGF were detected.

Statistical Analysis

GraphPad Prism 7.0 (Graph-Pad Software Inc., La Jolla, CA, USA) was utilized to perform statistical analyses. The difference between groups was analyzed by one-way analysis of variance (ANOVA) or Student's *t*-test. $P < 0.05$ were considered significant.

Results

Identification of Major Chemical Components in PS by UHPLC–MS/MS Analysis

A total of 223 compounds were identified in this study, including 147 compounds identified by positive spectrum and 76 compounds identified by negative spectrum. The total ion chromatograms (TICs) are shown in Figure 1A (positive ion mode) and 1B (negative ion mode). According to the similarity score of the spectrum, oral bioavailability (OB) > 30%, and drug resistance drug-likeness (DL) > 0.18, 28 main chemical components were finally screened. The detailed information of 28 compounds were shown in Table 2.

PS Improved Cardiac Structure and Function in AMI Rats

The study protocol is described in Figure 2A. To gain insights into the effects and mechanisms of PS against AMI, a rat model of AMI was established by ligating the LAD. Rats were treated continuously with the corresponding drugs according to the scheme for 4 weeks from the first day after surgery. Perindopril (0.84 mg/kg/d) was used as a positive drug control. At the same time, PX-478, an inhibitor of HIF-1α, was used to clarify the role of the miR-155/HIF-1α/

Table 1 Primer Sequences

Gene Symbol	Forward	Reverse
U6	CTCGCTTCGGCAGCACA	AACGCTTCACGAATTTGCGT
miR-155-5p	TCGGCAGGTTAATGCTAATTGTGAT	CTCAACTGGTGTCGTGGAGT
GAPDH	CGGAGTCAACGGATTTGGTCGTAT	AGCCTTCTCCATGGTGGTGAAGAC
HIF-1α	TGCTGGCTCCCTATATCCCA	TGCTGGCTCCCTATATCCCA
VEGF	AGGGCAGAATCATCACGAAGT	AGGGTCTCGATTGGATGGCA

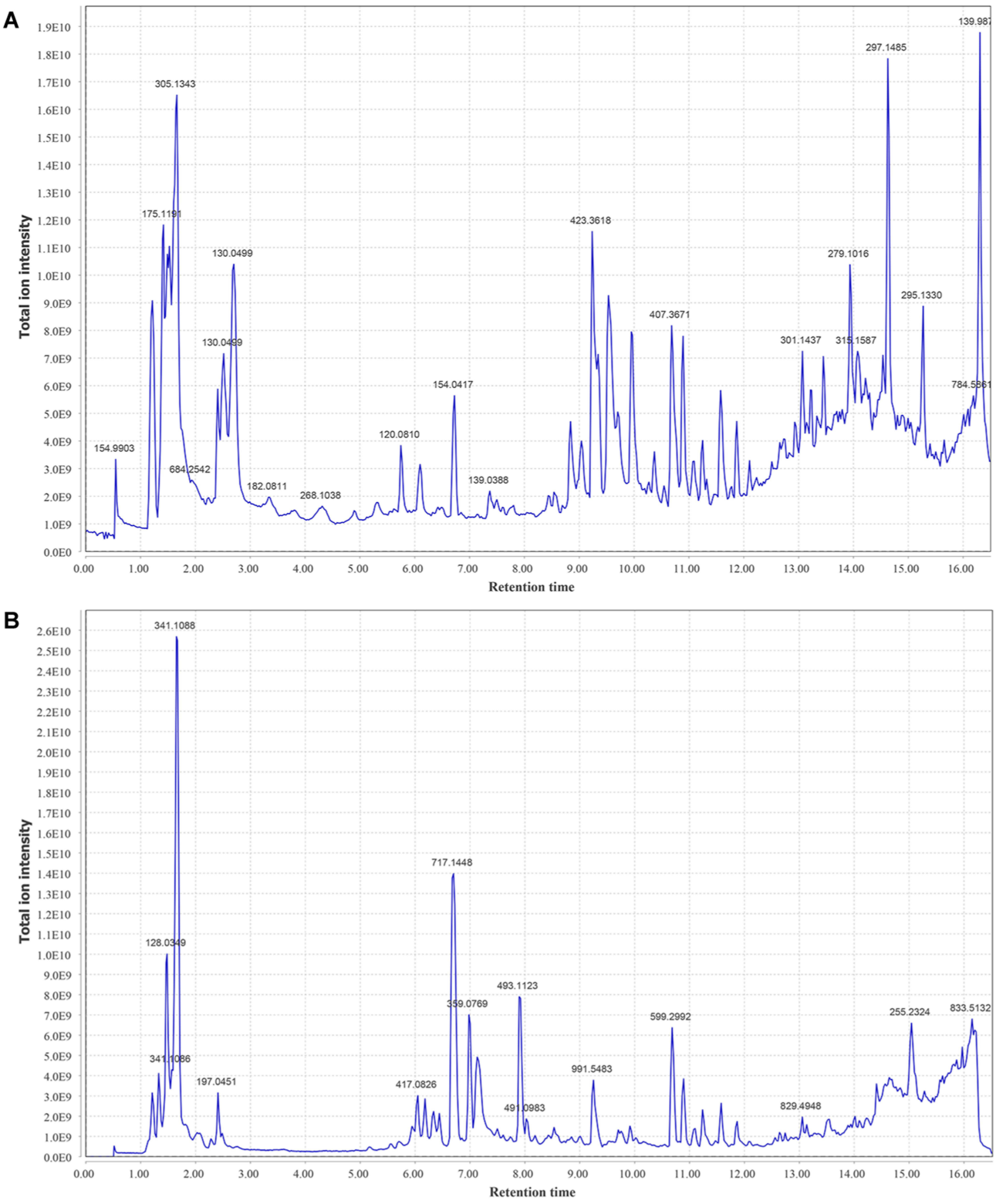

Figure 1 TICs of PS by UHPLC-MS/MS. (**A**) TIC of PS in positive ion mode. (**B**) TIC of PS in negative ion mode.

VEGF signaling pathway in the pro-angiogenic effect of PS in post-AMI rats. At the end of the study, 12 of 12 rats (100%) in the sham group survived, while 8 (66.67%), 9 (75%), 10 (83.33%), 10 (83.33%) and 11 (91.67%) rats in the model, PS-L, PS-H, PX-478 and ACEI groups survived respectively (Figure 2B).

Table 2 The Major Components of Panax Quinquefolium L. and Salvia Miltiorrhiza Bunge

ID	Name	Class	Chemical Formula	Chemical Structure	Pos/ Neg
M785T554_1	Ginsenoside F2		$C_{42}H_{72}O_{13}$	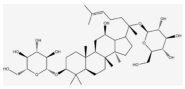	Pos
M287T808	Luteolin	Flavonoids	$C_{15}H_{10}O_6$	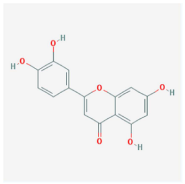	Pos
M287T481	Fisetin		$C_{15}H_{10}O_6$	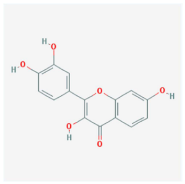	Pos
M303T508	Quercetin		$C_{15}H_{10}O_7$	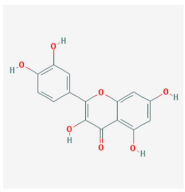	Pos
M433T501	Isovitexin		$C_{21}H_{20}O_{10}$	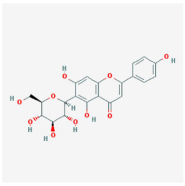	Pos
M272T535	Pelargonidin	Endogenous Metabolites	$C_{15}H_{11}O_5$	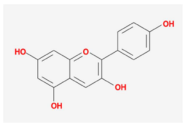	Pos

(*Continued*)

Table 2 (Continued).

ID	Name	Class	Chemical Formula	Chemical Structure	Pos/ Neg
M291T924	Sclareol	Prenol lipids	$C_{20}H_{36}O_2$	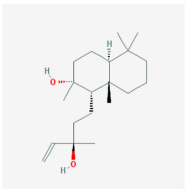	Pos
M303T578	Hesperetin	Flavonoids	$C_{16}H_{14}O_6$	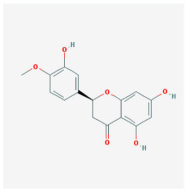	Pos
M336T622	Berberine	Protoberberine alkaloids and derivatives	$C_{20}H_{18}NO_4$	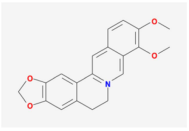	Pos
M373T751	Sinensetin	Flavonoids	$C_{20}H_{20}O_7$	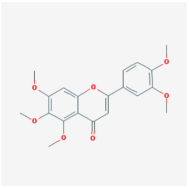	Pos
M383T977_3	Campesterol	Steroids and steroid derivatives	$C_{28}H_{48}O$	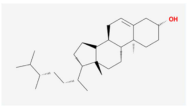	Pos
M403T793	Nobiletin	Flavonoids	$C_{21}H_{22}O_8$	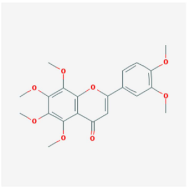	Pos

(*Continued*)

Table 2 (Continued).

ID	Name	Class	Chemical Formula	Chemical Structure	Pos/ Neg
M395T871	Alpha-Spinasterol	Steroids and steroid derivatives	$C_{29}H_{48}O$	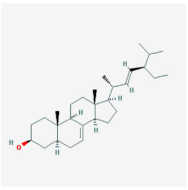	Pos
M447T606	Baicalin	Flavonoids	$C_{21}H_{18}O_{11}$	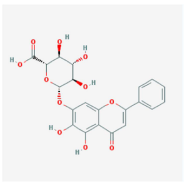	Pos
M283T924	Miltirone	Prenol lipids	$C_{19}H_{22}O_2$	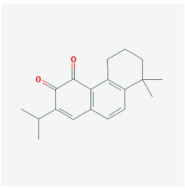	Pos
M785T573	Ginsenoside Rg3	Endogenous Metabolites; Natural Products/Medicines	$C_{42}H_{72}O_{13}$	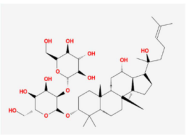	Pos
M308T624	Dihydrocapsaicin	Benzene and substituted derivatives	$C_{18}H_{29}NO_3$	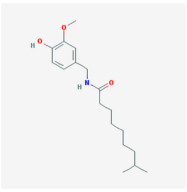	Pos
M427T561	Taraxerol	Prenol lipids	$C_{30}H_{50}O$	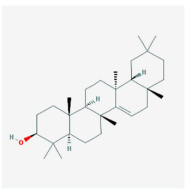	Pos

(*Continued*)

Table 2 (Continued).

ID	Name	Class	Chemical Formula	Chemical Structure	Pos/ Neg
M286T707	Kaempferol	Flavonoids	$C_{15}H_{10}O_6$	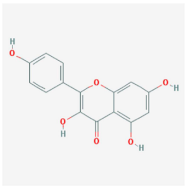	Neg
M283T604	Rhein	Anthracenes	$C_{15}H_8O_6$	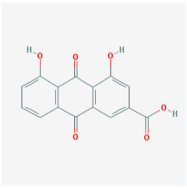	Neg
M283T628	Glycitein	Isoflavonoids	$C_{16}H_{12}O_5$	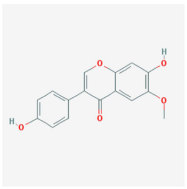	Neg
M267T655	Formononetin	Isoflavonoids	$C_{16}H_{12}O_4$	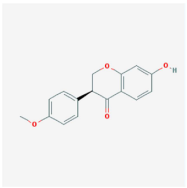	Neg
M269T608	Baicalein	Flavonoids	$C_{15}H_{10}O_5$	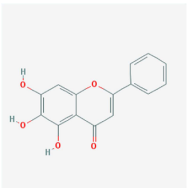	Neg
M289T432	Catechin	Flavonoids	$C_{15}H_{14}O_6$	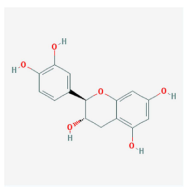	Neg

(*Continued*)

Table 2 (Continued).

ID	Name	Class	Chemical Formula	Chemical Structure	Pos/ Neg
M353T907	Yohimbine	Yohimbine alkaloids	$C_{21}H_{26}N_2O_3$	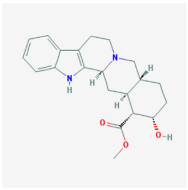	Neg
M269T371	Norizalpinin	Flavonoids	$C_{15}H_{10}O_5$	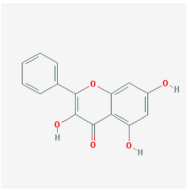	Neg
M269T633	Imperatorin	Coumarins and derivatives	$C_{16}H_{14}O_4$	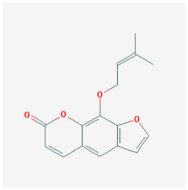	Neg
M593T608	Poncirin	Flavonoids	$C_{28}H_{34}O_{14}$	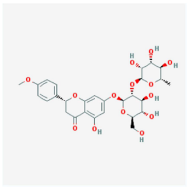	Neg

Echocardiography was used to assess cardiac structure and function, as described in Figure 2C, D. The echocardiographic parameters in the model group were characterized by lowered LVEF, LVFS, LVAWd, LVAWs, LVPWd and LVPWs and enlarged LVIDd and LVIDs, which indicated abnormal heart function and cardiac remodeling in contrast with the sham group ($P < 0.05$). As expected, both PS and ACEI markedly increased the LVEF, LVFS, LVAWd, LVAWs and LVPWs of AMI rats and decreased LVIDd and LVIDs ($P < 0.05$). Conversely, the function of PS mentioned above was strongly impaired by PX-478.

PS Reduced Myocardial Infarct Size in Rats with AMI

To observe the effect of PS on myocardial infarct size, the myocardial infarct area was evaluated by TTC staining (Figure 3A). The results demonstrated an obviously larger infarcted area in the model group than in the sham group ($P < 0.05$), and the above phenomena were partially reversed by PS and perindopril ($P < 0.05$). Moreover, the cardioprotective effects of PS were diminished by PX-478 in rats after AMI (Figure 3B).

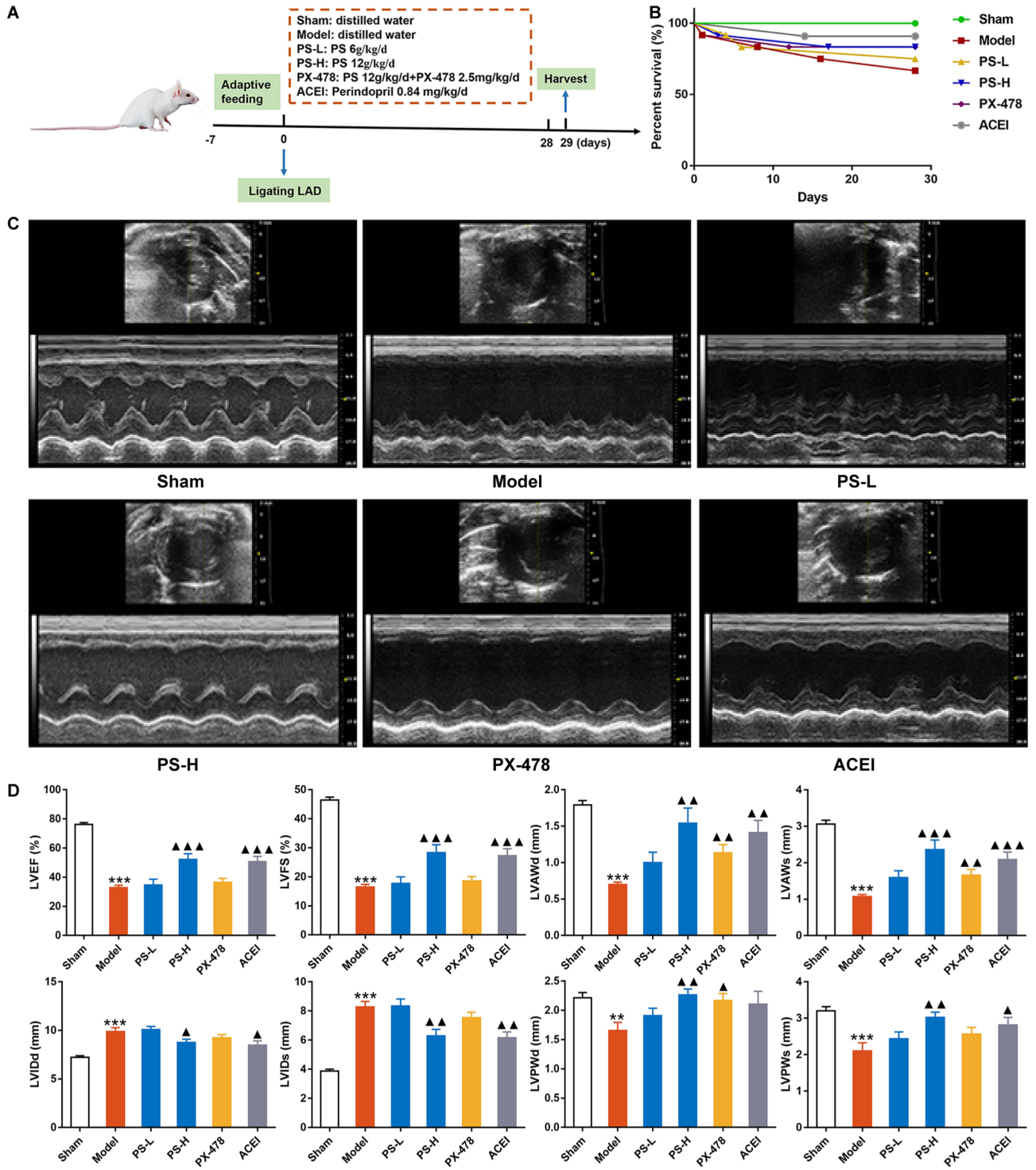

Figure 2 PS improved cardiac structure and function in AMI rats. (**A**) The study protocol of animal experiments; (**B**) The survival of experimental animals during the study period; (**C**) Representative echocardiographic images of rats in each group; (**D**) Quantification of cardiac function and structure. Data were expressed as the mean ± SEM, n=8. $^{**}P < 0.01$, $^{***}P < 0.001$, vs sham group; $^{▲}P < 0.05$, $^{▲▲}P < 0.01$, $^{▲▲▲}P < 0.001$, vs model group.

PS Relieved Histopathological Changes in Myocardial Tissues

H&E staining further revealed a reduced number of myocardial cells, hypertrophic and edematous cardiomyocytes, indistinct cytoplasmic borders and nuclei, and inflammatory cell infiltration in the model group in comparison to the sham group on day 28 post-AMI. However, when treated with PS, not only the number, shape and size of myocardial cells but also the infiltrated inflammatory cells were reversed by PS and perindopril compared with the model group (Figure 4A).

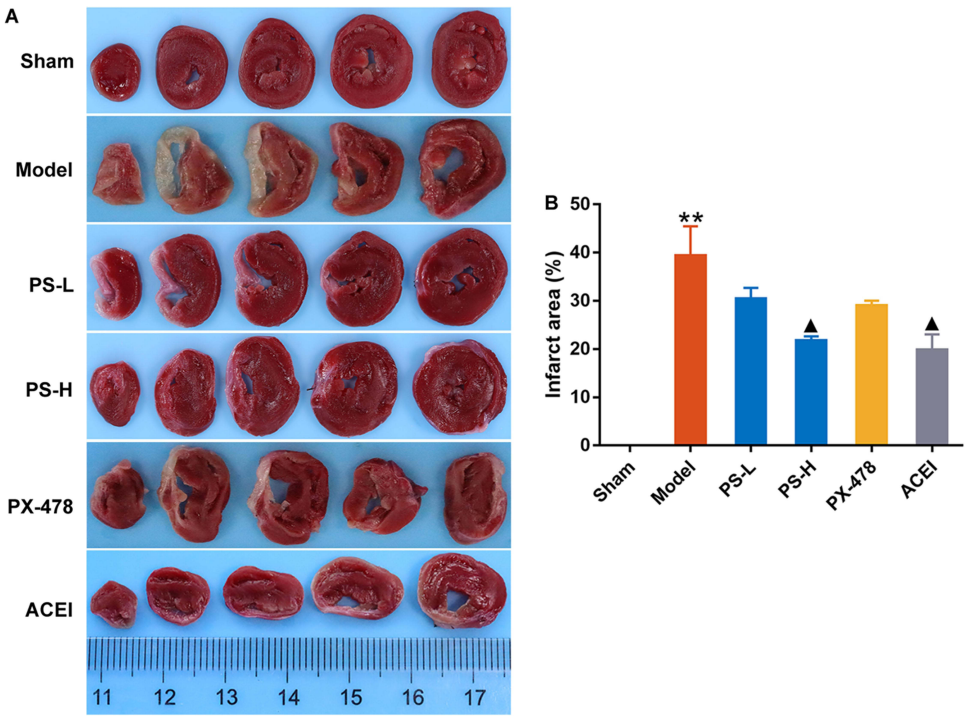

Figure 3 PS reduced myocardial infarct size in rats with AMI. (**A**) Representative TTC staining images of rats in each group; (**B**) Quantification of myocardial infarct size. Data were expressed as the mean ± SEM, n=3. ***P* < 0.01, vs sham group; ▲*P* < 0.05, vs model group.

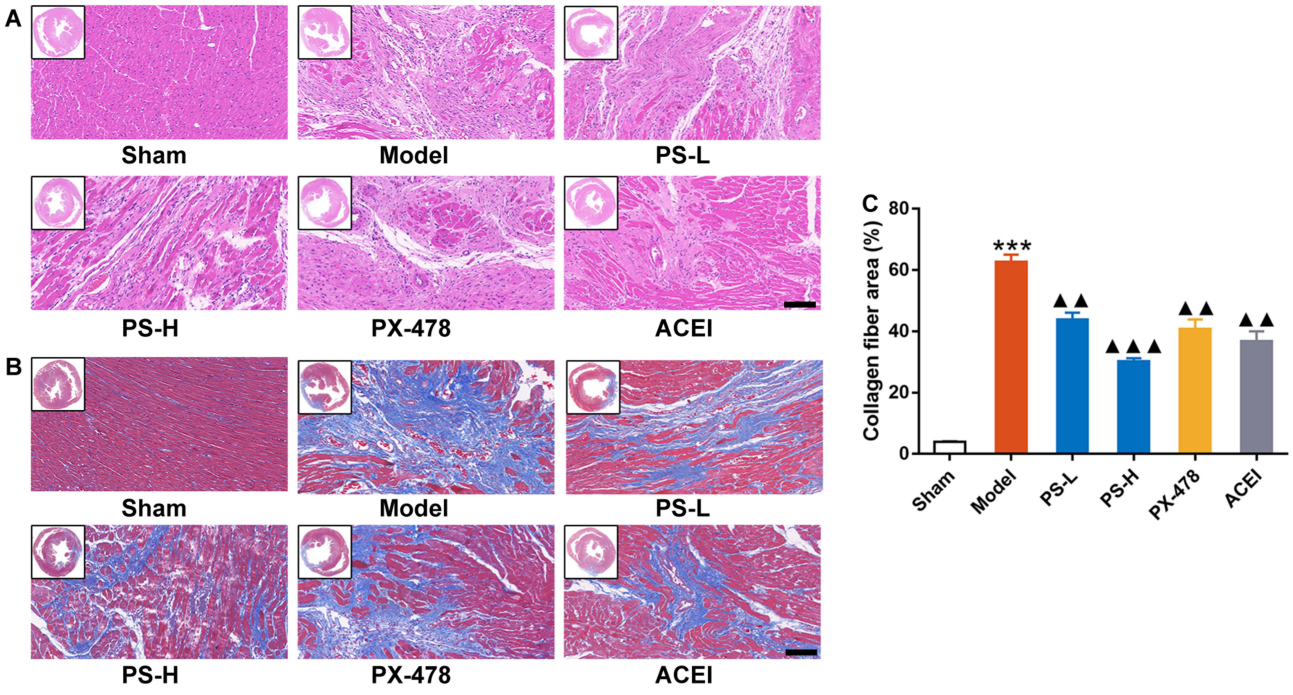

Figure 4 PS alleviated myocardial injury of AMI rats. (**A**) H&E staining of myocardial tissues, scale bar = 100 μm. (**B**) Masson staining of myocardial tissues, scale bar = 100 μm. (**C**) The percentage of collagen fiber area. Data were expressed as the mean ± SEM, n=3. ****P* < 0.001, vs sham group; ▲▲*P* < 0.01, ▲▲▲*P* < 0.001, vs model group.

https://doi.org/10.2147/DDDT.S426345

Likewise, Masson examination at 28 days after AMI suggested that collagen fiber deposition was significant in the model group compared with the sham group, and PS and perindopril further reduced AMI-induced collagen deposition in infarcted myocardium ($P < 0.05$) (Figure 4B and C). More intuitively, PX-478 reversed the effects of PS and perindopril on myocardial pathological changes.

PS Promoted Angiogenesis in Rats After AMI

Both MVD and CD31 are important proteins reflecting tissue angiogenesis. To identify the localization and expression of MVD and CD31, the marginal zone of myocardial infarction in rats after AMI was measured by immunohistochemical analysis. Representative images and quantitative results for each group are illustrated in Figure 5A and B. MVD and CD31 were localized in the nucleus and cytoplasm, and their expression was dark brown in immunohistochemical staining. The sham group and the model group showed significant differences in the expression levels of MVD and CD31 protein ($P < 0.05$). The levels of MVD and CD31 were appreciably increased in the PS-L, PS-H and ACEI groups compared with the model group ($P < 0.05$). However, the increase in MVD and CD31 induced by PS was partly inhibited by PX-478.

PS Increased the HGF and bFGF Levels in Serum

Angiogenic markers genes, such as HGF and bFGF are necessary for angiogenesis after AMI.[26] Therefore, we observed the effects of PS on the expression of these key cytokines involved in the activation of angiogenesis. As shown in Figure 6A, the high dose of PS and Perindopril administration markedly upregulated the level of HGF ($P < 0.05$). Moreover, this function of PS was weakened by PX-478. Regrettably, no significant difference was observed in the promoting effect of PS on bFGF (Figure 6B).

PS Inhibited the miR-155-5p/HIF-1α/VEGF Signaling Pathway in AMI Rats

Our previous work has shown that the mechanism of PS in treating coronary heart disease is related to angiogenesis in vivo, in which the HIF-1 signaling pathway and VEGF are key targets.[24] In addition, as an upstream regulatory gene of

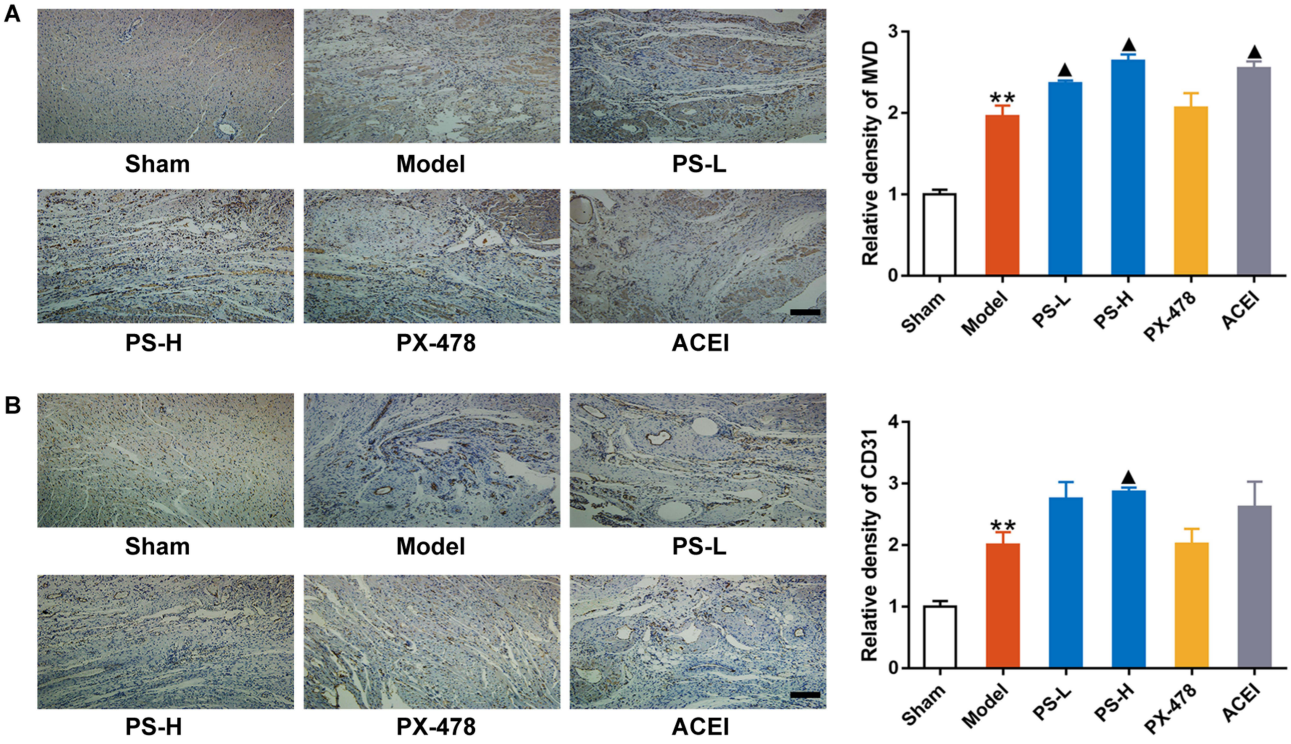

Figure 5 PS promoted the expression levels of MVD and CD31 in the marginal zone of myocardial infarction. (**A**) The expression of MVD. (**B**) The expression of CD31. Scale bar = 100 μm, data were expressed as the mean ± SEM, n=3. **$P < 0.01$, vs sham group; ▲$P < 0.05$, vs model group.

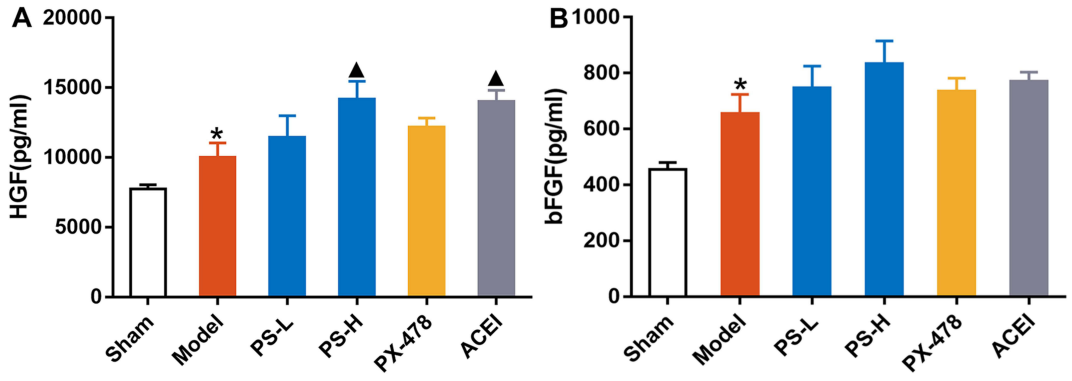

Figure 6 PS increased the expression level of HGF and bFGF in rats following an AMI. (**A**) The HGF level in serum, (**B**) The bFGF level in serum. Data were expressed as the mean ± SEM, n=8. *P < 0.05, vs sham group; ▲P < 0.05, vs model group.

HIF-1, miR-155 regulates endothelial cell proliferation and angiogenesis.[17] We speculated that the role of PS in promoting angiogenesis in rats after AMI was related to regulating the miR-155-5p/HIF-1α/VEGF signaling pathway. Thus, it is of great interest to identify whether PS is a potential regulator of the miR-155-5p/HIF-1α/VEGF axis. To this end, the mRNA and protein levels of HIF-1α and VEGF in the myocardial tissue of rats were detected (Figure 7).

We found that, as expected, PS significantly reduced the levels of miR-155-5p (P < 0.05) (Figure 7A). Then, when compared with the sham group, the mRNA and protein expression levels of HIF-1α were significantly elevated, while the mRNA and protein levels of VEGF were obviously decreased in the AMI group (P < 0.05) (Figure 7B–E). Instead, PS and perindopril inhibited the mRNA and protein expression levels of HIF-1α and enhanced the levels of VEGF (P < 0.05) (P < 0.05) (Figure 7B–E). Moreover, the HIF-1α inhibitor PX-478, was used to further clarify whether the effect of PS on promoting angiogenesis is mediated by HIF-1α/VEGF. Excitingly, PX-478 partially reversed the above regulatory effects of

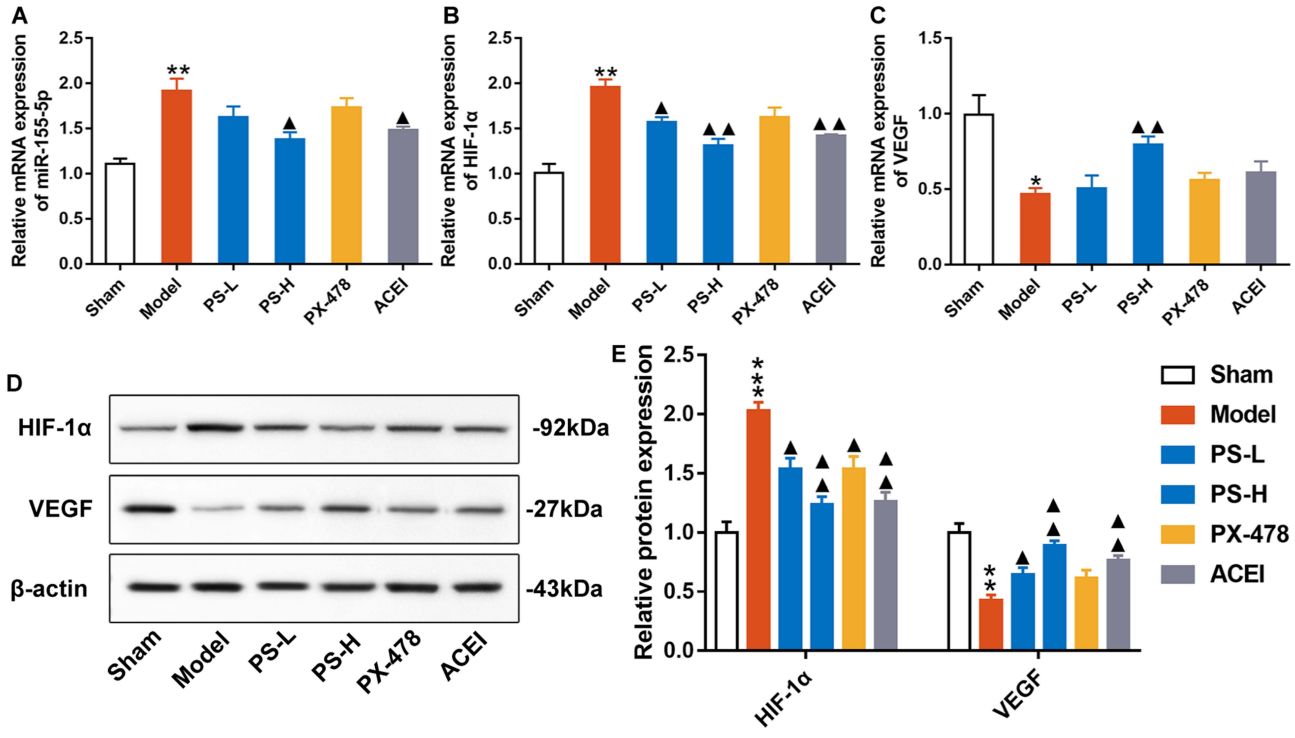

Figure 7 PS inhibited the miR-155-5p/HIF-1 α/VEGF signaling pathway in AMI rats. (**A**) The relative mRNA expression of miRNA-155-5p in myocardial tissues, (**B**) The relative mRNA expression of HIF-1 α in myocardial tissues, (**C**) The relative mRNA expression of VEGF in myocardial tissues, (**D**) Representative immunoblot band diagram immunoblots against HIF-1 α and VEGF in myocardial tissues, (**E**) Quantitative values of HIF-1 α and VEGF relative protein expression in myocardial tissue. Data were expressed as the mean ± SEM, n=3. *P < 0.05, **P < 0.01, ***P < 0.001, vs sham group; ▲P < 0.05, ▲▲P < 0.01, vs model group.

PS. The inhibitory effect of PS on promoting angiogenesis was mediated by the miR-155-5p/HIF-1α/VEGF signaling pathway in rats after AMI.

Discussion

This study presented several novel findings. First, PS reduced the myocardial infarction area and improved cardiac function in rats with AMI. Second, PS promoted angiogenesis in post-AMI rats, and its mechanism was related to regulating the miR-155-5p/HIF-1α/VEGF pathway. Third, PX-478, an inhibitor of HIF-1α, weakened the effect of PS above. PS may be an attractive drug candidate for the treatment of AMI.

TCM has a long history in treating various diseases. Qi deficiency and blood stasis are accepted as the main pathogenesis in ischemic heart disease according to TCM theories.[27] PS is a compatibility scheme of TCM for tonifying qi and activating blood. Modern pharmacological studies have revealed that PS and their active ingredients promoted angiogenesis in rats with AMI, which may be related to the upregulation of VEGF and bFGF.[28,29] Through network pharmacology, we also found that PS regulated angiogenesis of coronary heart disease and is related to HIF-1/VEGF pathway.[24] Based on the above analysis, the role and mechanism of PS on angiogenesis after AMI are of great importance. In the present study, an AMI rat model was established by ligation of the LAD. Rats in the model group exhibited ventricular remodeling, which was characterized by the enlargement of the ventricular cavity and the thinning of the ventricular wall. Then, the model group showed a remarkable elevation in myocardial infarction area. In addition, histopathology was suggestive of extensive myocyte necrosis, intense inflammatory cell infiltrates and abundant collagen fibers in the model group. However, PS improved cardiac structure and function, reduced infarct size, and alleviated myocardial fibrosis and inflammatory cell infiltration in rats following AMI.

The term "angiogenesis" was originally introduced by the British surgeon John Hunter in 1787,[30] which is a process of generating new capillaries from preexisting vessels in the form of budding or nonbudding by the proliferation and migration of vascular endothelial cells based on the original vascular bed.[31,32] Therapeutic angiogenesis promotes angiogenesis of ischemic myocardium, and establishing effective collateral circulation are critical for the recovery of cardiac function after AMI.[33] Thus, proangiogenesis is generally considered to be an effective therapeutic strategy for treating AMI. FGF and bFGF are known as powerful angiogenesis factors, which increases the proliferation and migration of endothelial cells.[34,35] MVD refers to the number of microvessels per unit of tissue volume, or the number of microvessels per unit of tissue cross-sectional area.[36] Furthermore, CD31 is a specific marker of angiogenesis.[37] In the current study, AMI-induced impaired angiogenesis was confirmed by the marked elevation of MVD and CD31 in myocardial tissues, as well as HGF and bFGF in serum. However, PS reversed the above changes and promoted angiogenesis.

miRNA is a class of noncoding small RNA molecules consisting of 21–23 nucleotides, and a key inhibitor of gene expression by binding to the 3′- untranslated region (UTR) of target mRNA.[38] miR-155-5p inhibition rejuvenates aged mesenchymal stem cells and enhances angiogenesis, thus playing a cardioprotective role after AMI.[39] HIFs have been identified as a group of highly conserved factors that control the expression of many angiogenesis genes.[40] VEGF is an effective mitogen and important proangiogenic factor.[41] It promotes an increase in vascular permeability, degeneration of extracellular matrix, vascular endothelial cell migration and proliferation, and induction of angiogenesis.[42] It has been proven to promote angiogenesis in vivo models.[43] Indeed, HIF-1α is induced in endothelial cells, resulting in the activation of VEGF and its receptor gene transcription.[44] In this study, we explored the role and mechanism of the miR-155/HIF-1α/VEGF pathway in mediating the effect of PS on angiogenesis in the ischemic myocardium following an AMI. To better clarify this mechanism, PX-478, a HIF-1α inhibitor, was used. The mRNA level of miR-155-5p was enhanced in the model group and was reduced by PS.

Moreover, after continuous treatment with PS throughout the process, the mRNA and protein levels of HIF-1α significantly decreased, while those of VEGF increased compared with those in the model group. The above regulatory effects of PS on the miR-155-5p/HIF-1α/VEGF pathway were reversed by PX-478. Considering these results, we inferred that PS could regulate the miR-155-5p/HIF-1α/VEGF axis, promoting angiogenesis, which is an effective drug for AMI.

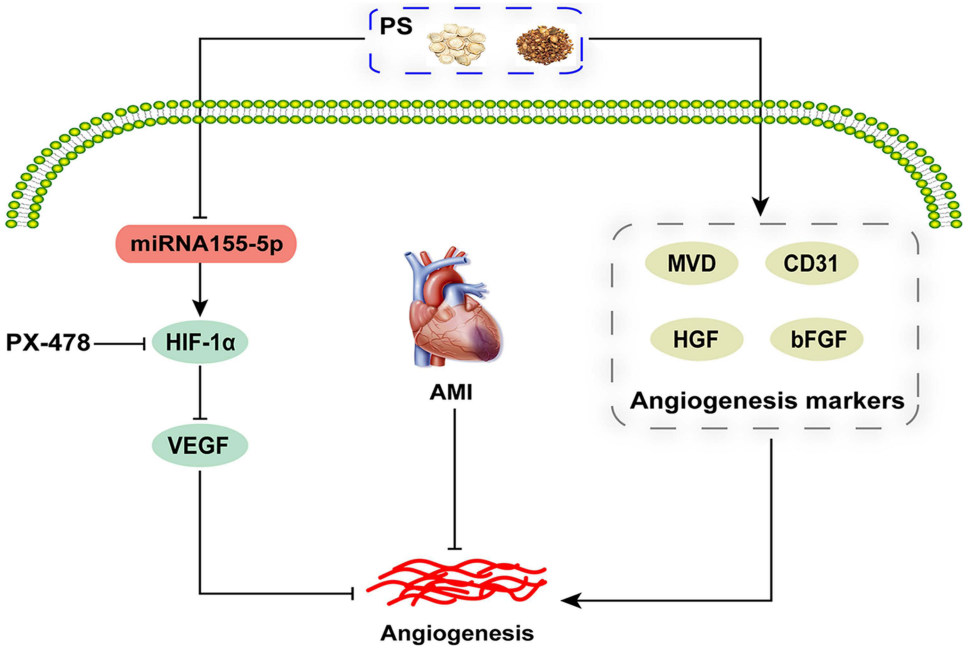

Figure 8 PS enhances angiogenesis by regulating the miR-155-5p/HIF-1α/VEGF axis in acute myocardial infarction.

Conclusion

In brief, our study indicated that PS promoted angiogenesis by inhibiting the miR-155-5p/HIF-1α/VEGF signaling pathway, thereby reducing the myocardial infarction area and improving cardiac function in rats following AMI. These results not only from our deeper understanding of the mechanism of PS in the treatment of AMI but also offer laboratory evidence for optimizing innovative drug candidates based on PS and using them as the main or adjuvant therapy for AMI (Figure 8).

Acknowledgments

This work was supported by grants from Beijing University of Chinese Medicine New Teacher Launch Fund Project (2022-JYB-XJSJJ-073) and National Natural Science Foundation of China (81573900).

Disclosure

The authors report no conflicts of interest in this work.

References

1. Virani SS, Alonso A, Benjamin EJ., et al. Heart disease and stroke statistics-2020 update: a report from the American Heart Association. *Circulation*. 2020;141(9):e139–e596. doi:10.1161/CIR.0000000000000757
2. Xue J, Chen L, Cheng H, et al. The identification and validation of hub genes associated with acute myocardial infarction using weighted gene co-expression network analysis. *J Cardiovasc Dev Dis*. 2022;9(1):30. doi:10.3390/jcdd9010030
3. Ylä-Herttuala S, Bridges C, Katz MG, Korpisalo P. Angiogenic gene therapy in cardiovascular diseases: dream or vision? *Eur Heart J*. 2017;38(18):1365–1371. doi:10.1093/eurheartj/ehw547
4. Faris P, Negri S, Perna A, Rosti V, Guerra G, Moccia F. Therapeutic potential of endothelial colony-forming cells in ischemic disease: strategies to improve their regenerative efficacy. *Int J Mol Sci*. 2020;21(19):7406. doi:10.3390/ijms21197406
5. Shyu KG, Wang BW, Fang WJ, Pan CM, Lin CM. Hyperbaric oxygen-induced long non-coding RNA MALAT1 exosomes suppress microRNA-92a expression in a rat model of acute myocardial infarction. *J Cell Mol Med*. 2020;24(22):12945–12954. doi:10.1111/jcmm.15889
6. Zhai S, Zhang XF, Lu F, et al. Chinese medicine GeGen-DanShen extract protects from myocardial ischemic injury through promoting angiogenesis via up-regulation of VEGF/VEGFR2 signaling pathway. *J Ethnopharmacol*. 2021;267(2021):113475. doi:10.1016/j.jep.2020.113475
7. Nazari A, Chehelcheraghi F. Using apelin and exercise to protect the cardiac cells: synergic effect in ischemia reperfusion injuries treatment in rats. *Bratisl Lek Listy*. 2020;121(1):14–21. doi:10.4149/BLL_2020_003
8. Wang Y, Zhao R, Liu D, Deng W. Exosomes derived from miR-214-enriched bone marrow-derived mesenchymal stem cells regulate oxidative damage in cardiac stem cells by targeting CaMKII. *Oxid Med Cell Longev*. 2018;2018:4971261. doi:10.1155/2018/4971261
9. Zhou Z, Lu Y, Wang Y, Du L, Zhang Y, Tao J. Let-7c regulates proliferation and osteodifferentiation of human adipose-derived mesenchymal stem cells under oxidative stress by targeting SCD-1. *Am J Physiol Cell Physiol*. 2019;316(1):c57–69. doi:10.1152/ajpcell.00211.2018

10. Yang D, Wang J, Xiao M, Zhou T, Shi X. Role of mir-155 in controlling HIF-1α level and promoting endothelial cell maturation. *Sci Rep*. 2016;6 (1):35316. doi:10.1038/srep35316
11. Koyasu S, Kobayashi M, Goto Y, Hiraoka M, Harada H. Regulatory mechanisms of hypoxia-inducible factor 1 activity: two decades of knowledge. *Cancer Sci*. 2018;109(3):560–571. doi:10.1111/cas.13483
12. Yu J, Zhang L, Zhang H. Atorvastatin combined with routine therapy on HIF-1, VEGF concentration and cardiac function in rats with acute myocardial infarction. *Exp Ther Med*. 2020;19(3):2053–2058. doi:10.3892/etm.2020.8438
13. Korbecki J, Kojder K, Kapczuk P, Kupnicka P. The effect of hypoxia on the expression of CXC chemokines and CXC chemokine receptors-a review of literature. *Int J Mol Sci*. 2021;22(2):843. doi:10.3390/ijms22020843
14. Shi Y, Liu Z, Zhang Q. Phosphorylation of seryl-tRNA synthetase by ATM/ATR is essential for hypoxia-induced angiogenesis. *PLoS Biol*. 2020;18 (12):e3000991. doi:10.1371/journal.pbio.3000991
15. Tompkins BA, Balkan W, Winkler J, et al. Preclinical studies of stem cell therapy for heart disease. *Circ Res*. 2018;122(7):1006–1020. doi:10.1161/CIRCRESAHA.117.312486
16. Wang J, Zou Y, Du B, et al. SNP-mediated lncRNA-ENTPD3-AS1 upregulation suppresses renal cell carcinoma via miR-155/HIF-1α signaling. *Cell Death Dis*. 2021;12(7):672. doi:10.1038/s41419-021-03958-4
17. Chen JG, Xu XM, Ji H, Sun B. Inhibiting miR-155 protects against myocardial ischemia/reperfusion injury via targeted regulation of HIF-1α in rats. *Iran J Basic Med Sci*. 2019;22(9):1050–1058. doi:10.22038/ijbms.2019.34853.8270
18. Zhu J, Zhang X, Gao W, Hu H, Wang X, Hao D. lncRNA/circRNA-miRNA-mRNA ceRNA network in lumbar intervertebral disc degeneration. *Mol Med Rep*. 2019;20(4):3160–3174. doi:10.3892/mmr.2019.10569
19. Sun CY, Zhang XP, Liu F, Wang W. Orchestration of lincRNA-p21 and miR-155 in modulating the adaptive dynamics of HIF-1α. *Front Genet*. 2020;11:871. doi:10.3389/fgene.2020.00871
20. Li DD. Study on the mechanism of intervention of American Ginseng and Salvia Miltiorrhiza on thrombosis. Beijing: China Academy of Chinese Medical Sciences [Master thesis]; 2019.
21. Lin Q. *Study on the Mechanism of the Combination of American Ginseng and Salvia Miltiorrhiza in Stabilizing Vulnerable Atherosclerotic Plaques by Regulating PI3K/Akt/NF-κB Pathway* [Doctor thesis]. Beijing: China Academy of Chinese Medical Sciences; 2021.
22. Ruan H, Hu TH, Ma XJ, Miao Y, Li DD, Yin HJ. Study on the antithrombotic mechanism of Yiqi Huoxue compound. *Chin J Evid Based Cardiovasc Med*. 2019;11(4):410–417.
23. Zhang M. *Clinical Evaluation of the Treatment of Cardiovascular Diseases with Yiqi Huoxue Method Based on Meta Analysis and Data Mining* [Doctor thesis]. Beijing: Beijing University of Chinese Medicine; 2019.
24. Lin Q, Xu FQ, Ma XJ, Wang Z, Li DD, Yin HJ. Study on the mechanism of American Ginseng Salvia Miltiorrhiza in treating coronary heart disease based on network pharmacology. *Chin J Integr Med Cardio*. 2021;19(11):1777–1787.
25. Goldman S, Raya TE. Rat infarct model of myocardial infarction and heart failure. *J Card Fail*. 1995;1(2):169–177. doi:10.1016/1071-9164(95)90019-5
26. Wang L, Pasha Z, Wang S, et al. Protein kinase G1 α overexpression increases stem cell survival and cardiac function after myocardial infarction. *PLoS One*. 2013;8(3):e60087. doi:10.1371/journal.pone.0060087
27. Gao ZY, Xu H, Shi DZ, Wen C, Liu BY. Analysis on outcome of 5284 patients with coronary artery disease: the role of integrative medicine. *J Ethnopharmacol*. 2012;141(2):578–583. doi:10.1016/j.jep.2011.08.071
28. Chen J, Wang Y, Wang S, Zhao X, Zhao L, Wang Y. Salvianolic acid B and ferulic acid synergistically promote angiogenesis in HUVECs and zebrafish via regulating VEGF signaling. *J Ethnopharmacol*. 2022;283:114667. doi:10.1016/j.jep.2021.114667
29. Yin Y, Duan J, Guo C, et al. Danshensu accelerates angiogenesis after myocardial infarction in rats and promotes the functions of endothelial progenitor cells through SDF-1α/CXCR4 axis. *Eur J Pharmacol*. 2017;814:274–282. doi:10.1016/j.ejphar.2017.08.035
30. Lenzi P, Bocci G, Natale G. John Hunter and the origin of the term "angiogenesis". *Angiogenesis*. 2016;19(2):255–256. doi:10.1007/s10456-016-9496-7
31. Bosisio D, Salvi V, Gagliostro V, Sozzani S. Angiogenic and antiangiogenic chemokines. *Chem Immunol Allergy*. 2014;99:89–104.
32. Ma Q, Reiter RJ, Chen Y. Role of melatonin in controlling angiogenesis under physiological and pathological conditions. *Angiogenesis*. 2020;23 (2):91–104. doi:10.1007/s10456-019-09689-7
33. Moccia F, Negri S, Faris P, Ronchi C, Lodola F. Optical excitation of organic semiconductors as a highly selective strategy to induce vascular regeneration and tissue repair. *Vascul Pharmacol*. 2022;144:106998. doi:10.1016/j.vph.2022.106998
34. Alexander SPH, Fabbro D, Kelly E. THE CONCISE GUIDE TO PHARMACOLOGY 2019/20: catalytic receptors. *Br J Pharmacol*. 2019;176 (Suppl 1):s247–s296. doi:10.1111/bph.14751
35. Przybylski M. A review of the current research on the role of bFGF and VEGF in angiogenesis. *J Wound Care*. 2009;18(12):516–519. doi:10.12968/jowc.2009.18.12.45609
36. Huxley VH, Kemp SS. Sex-specific characteristics of the microcirculation. *Adv Exp Med Biol*. 2018;1065:307–328.
37. Li Z, Fan H, Cao J, et al. Natriuretic peptide receptor a promotes gastric malignancy through angiogenesis process. *Cell Death Dis*. 2021;12 (11):968. doi:10.1038/s41419-021-04266-7
38. Xu R, Shen X, Si Y, et al. MicroRNA-31a-5p from aging BMSCs links bone formation and resorption in the aged bone marrow microenvironment. *Aging Cell*. 2018;17(4):e12794. doi:10.1111/acel.12794
39. Hong Y, He H, Jiang G, et al. miR-155-5p inhibition rejuvenates aged mesenchymal stem cells and enhances cardioprotection following infarction. *Aging Cell*. 2020;19(4):e13128. doi:10.1111/acel.13128
40. Krock BL, Skuli N, Simon MC. Hypoxia-induced angiogenesis: good and evil. *Genes Cancer*. 2011;2(12):1117–1133. doi:10.1177/1947601911423654
41. Guo X, Yi H, Li TC, Wang Y, Wang H, Chen X. Role of vascular endothelial growth factor (VEGF) in human embryo implantation: clinical implications. *Biomolecules*. 2021;11(2):253. doi:10.3390/biom11020253
42. Eguchi R, Kawabe JI, Wakabayashi I. VEGF-independent angiogenic factors: beyond VEGF/VEGFR2 signaling. *J Vasc Res*. 2022;59(2):78–89. doi:10.1159/000521584
43. Dvorak HF. VPF/VEGF and the angiogenic response. *Semin Perinatol*. 2000;24(1):75–78. doi:10.1016/S0146-0005(00)80061-0
44. Tang N, Wang L, Esko J, et al. Loss of HIF-1alpha in endothelial cells disrupts a hypoxia-driven VEGF autocrine loop necessary for tumorigenesis. *Cancer Cell*. 2004;6(5):485–495. doi:10.1016/j.ccr.2004.09.026